OPEN ACCESS
OPUS AUGSBURG

Universität Augsburg
Universitätsbibliothek

Evidence of Fukushima fallout in the area affected by wildfires in Kamaishi (Iwate Prefecture, Tohoku Region, Japan): implications for future environmental research using radionuclide tracers

Olivier Evrard, Naoya Takahashi, Hotaka Sato, Ryoga Ohta, Anthony Foucher, Thomas Chalaux-Clergue, Pierre-Alexis Chaboche

Angaben zur Veröffentlichung / Publication details:

Evrard, Olivier, Naoya Takahashi, Hotaka Sato, Ryoga Ohta, Anthony Foucher, Thomas Chalaux-Clergue, and Pierre-Alexis Chaboche. 2026. “Evidence of Fukushima fallout in the area affected by wildfires in Kamaishi (Iwate Prefecture, Tohoku Region, Japan): implications for future environmental research using radionuclide tracers.” Journal of Environmental Radioactivity 292: 107876. https://doi.org/10.1016/j.jenvrad.2025.107876.

Nutzungsbedingungen / Terms of use: **CC BY 4.0**

Dieses Dokument wird unter folgenden Bedingungen zur Verfügung gestellt: / This document is made available under these conditions:
CC-BY 4.0: Creative Commons: Namensnennung
Weitere Informationen finden Sie unter: / For more information see:
https://creativecommons.org/licenses/by/4.0/deed.de

Journal of Environmental Radioactivity 292 (2026) 107876

Contents lists available at ScienceDirect

Journal of Environmental Radioactivity

journal homepage: www.elsevier.com/locate/jenvrad

Evidence of Fukushima fallout in the area affected by wildfires in Kamaishi (Iwate Prefecture, Tohoku Region, Japan): Implications for future environmental research using radionuclide tracers

Olivier Evrard [a,b,*], Naoya Takahashi [c], Hotaka Sato [c], Ryoga Ohta [d], Anthony Foucher [b], Thomas Chalaux-Clergue [e], Pierre-Alexis Chaboche [f,g]

[a] MITATE Lab Post-Fukushima Studies, International Research Laboratory 2039 (CNRS, CEA, Fukushima University), Fukushima, Japan
[b] Laboratoire des Sciences Du Climat et de L'Environnement (LSCE, IPSL), Unité Mixte de Recherche 8212 (CEA, CNRS, UVSQ), Université Paris-Saclay, Gif-sur-Yvette, France
[c] Department of Earth Science, Tohoku University, Sendai, Japan
[d] Faculty of Humanities, Niigata University, Niigata, Japan
[e] Working Group Water and Soil Resource Research, University of Augsburg, Augsburg, Germany
[f] International Research Fellow of Japan Society for the Promotion of Science, Postdoctoral Fellowships for Research in Japan (Standard), Japan
[g] Institute of Environmental Radioactivity (IER), University of Fukushima, Fukushima, Japan

ARTICLE INFO

Keywords:
Radiocesium
^{134}Cs
^{137}Cs
^{210}Pb$_{xs}$
Fingerprinting
Soil inventories

ABSTRACT

Significant deposition of radiocesium including ^{134}Cs and ^{137}Cs occurred in March 2011 following the Fukushima nuclear accident across vast regions of Northeastern Japan. However, as most studies focused on fallout that took place in the Fukushima Prefecture, much less information is available on the situation that prevails further to the North, in other parts of the Tohoku Region of Japan. In this context, the current research investigated the occurrence of fallout radionuclides (including natural ^{210}Pb$_{xs}$ as well as artificial ^{134}Cs and ^{137}Cs) in burned and unburned soil profiles as well as in a range of surface soil and sediment samples collected in the region of Kamaishi (Iwate Prefecture, Tohoku Region, Japan) affected by wildfires in 2017. Results show that ^{210}Pb$_{xs}$ and ^{137}Cs may be used as tracers of sediment sources across landscapes affected by wildfires in this region. Furthermore, the soil profile analysis demonstrated that all analysed fallout radionuclides were found enriched in the burned vs. unburned profiles, due to the incorporation of radionuclides trapped by vegetation into the ash after the fire. The detection of ^{134}Cs in the uppermost 0–5 cm depth layer in all investigated soil profiles also allowed to demonstrate the occurrence of significant Fukushima fallout of ^{134}Cs and ^{137}Cs in this region (roughly of the same order of magnitude as the fallout associated with the nuclear atmospheric tests in the 1960s). In the future, both sources of fallout should be considered to provide relevant interpretations when examining radionuclide data found in environmental samples collected in vast regions of Northeastern Japan. The analysis of ^{134}Cs should also be encouraged to document the sources of fallout in these regions as long as this short-lived radionuclide remains detectable (i.e., theoretically by 2031).

1. Introduction

Following the Fukushima Dai-ichi Nuclear Power Plant (FDNPP) accident in March 2011, airborne surveys were rapidly available as soon as in April 2011 to document the spatial variations of radionuclide deposition across Northeastern Japan (Kato et al., 2019; Masson et al., 2011) (Fig. 1a). Most of deposition consisted of radiocesium including ^{134}Cs and ^{137}Cs ($T_{1/2}$ = 2.064 years and 30.018 years, respectively) (Shozugawa et al., 2012; Steinhauser et al., 2014). Both isotopes were emitted in similar proportions at the moment of the accident (Kobayashi et al., 2015) although they decay with very different velocities, given their contrasting half-lives. Most monitoring efforts were logically concentrated across the main radioactive plume located to the north-west of FDNPP (Fig. 1a), and within Fukushima Prefecture (Evrard et al., 2015; Onda et al., 2020). Although it is known from airborne surveys and other measurements (e.g. foodstuff analyses) that significant

* Corresponding author. MITATE Lab Post-Fukushima Studies, International Research Laboratory 2039 (CNRS, CEA, Fukushima University), Fukushima, Japan.
E-mail address: olivier.evrard@lsce.ipsl.fr (O. Evrard).

https://doi.org/10.1016/j.jenvrad.2025.107876
Received 20 November 2025; Received in revised form 6 December 2025; Accepted 8 December 2025
Available online 11 December 2025
0265-931X/© 2025 The Authors. Published by Elsevier Ltd. This is an open access article under the CC BY license (http://creativecommons.org/licenses/by/4.0/).

radioactive fallout took place in other Prefectures of Northeastern Japan (Hori et al., 2018), more precise measurements are lacking in some of these areas, particularly in the northern part of Tohoku Region, in order to verify the occurrence and quantify the magnitude of Fukushima fallout in these regions.

Still, as fallout radionuclides including artificial ^{137}Cs are increasingly used as temporal markers or sediment source tracers in Earth Science and environmental research (Evrard et al., 2020; Mabit et al., 2008), it is of paramount importance to determine unambiguously whether radioactive fallout occurred in these regions following FDNPP accident in 2011 along with its potential magnitude. Indeed, several decades after Chernobyl accident that took place in 1986, numerous publications continue to attribute ^{137}Cs peaks recorded in sediment archives to this accident in areas that are very unlikely to be affected by Chernobyl fallout (Foucher et al., 2021), due to this lack of unambiguous determination of those areas affected by post-accidental fallout. Such reconstruction of initial radiocesium deposition remains possible several decades after the emission event (Meusburger et al., 2020), although it requires the deployment of time-consuming and expensive experiments to analyse other longer-lived isotopes such as those of plutonium or long-lived ^{135}Cs (Jaegler et al., 2018; Magre et al., 2022; Steinhauser, 2014). To avoid these time-consuming and destructive analyses, the measurement of traces of ^{134}Cs that may only have been emitted into the environment by FDNPP accident in Japan during the 21st century before its complete decay (estimated to take place after ~10 half-lives, i.e. by 2031 for FDNPP accident) may provide an effective alternative to investigate the occurrence of Fukushima-related radiocesium fallout across vast areas in Northeastern Japan.

In addition to providing chronological markers used for dating sediment archives (Bruel and Sabatier, 2020), fallout radionuclides supplied to the soil with rainfall are also often used to distinguish between contrasted sediment source contributions from the landscape. Typically, they allow differentiating the respective proportions of material originating from surface sources exposed and enriched in fallout radionuclides and those of subsoil material (i.e., rills, gullies, channel banks, landslides) depleted in radioisotopes (Evrard et al., 2020), which is particularly useful to identify the main soil erosion processes.

As fallout radionuclides provide useful tracers of sediment redistribution following environmental disturbances (Owens, 2020), an area of specific interest in Japan was the zone affected by extensive wildfires near Kamaishi City, in Iwate Prefecture. These fires took place in May 2017 and burned a surface area of 413 ha, which was at that time the largest forest fire in Japan that occurred since 1995 and which may be considered as an extreme fire in Japan as the affected area was higher than the total area generally affected by fires nationwide – 384 ha in 2016 (Touge et al., 2023). It has indeed been shown that wildfires lead to the concentration of radionuclides (mainly the natural ^{210}Pb in addition to ^{137}Cs) accumulated over time by the vegetation and organic matter in ash, which may then be used to trace sediment redistribution and source contributions following such disasters (Estrany et al., 2016; Smith et al., 2011).

In this context, the current research will investigate the potential occurrence of Fukushima-related radiocesium deposition in 2011 in the area affected by wildfires in Kamaishi City, Northern Japan. It will also determine whether fallout radionuclides may provide useful tracers of sediment redistribution following wildfires in this region of Northern Japan through the comparison of radionuclide activities in soil profiles collected in burned vs. unburned areas. Finally, the potential use of fallout radionuclides to quantify surface vs. subsurface sediment source contributions in such a context of environmental disturbance will also be discussed.

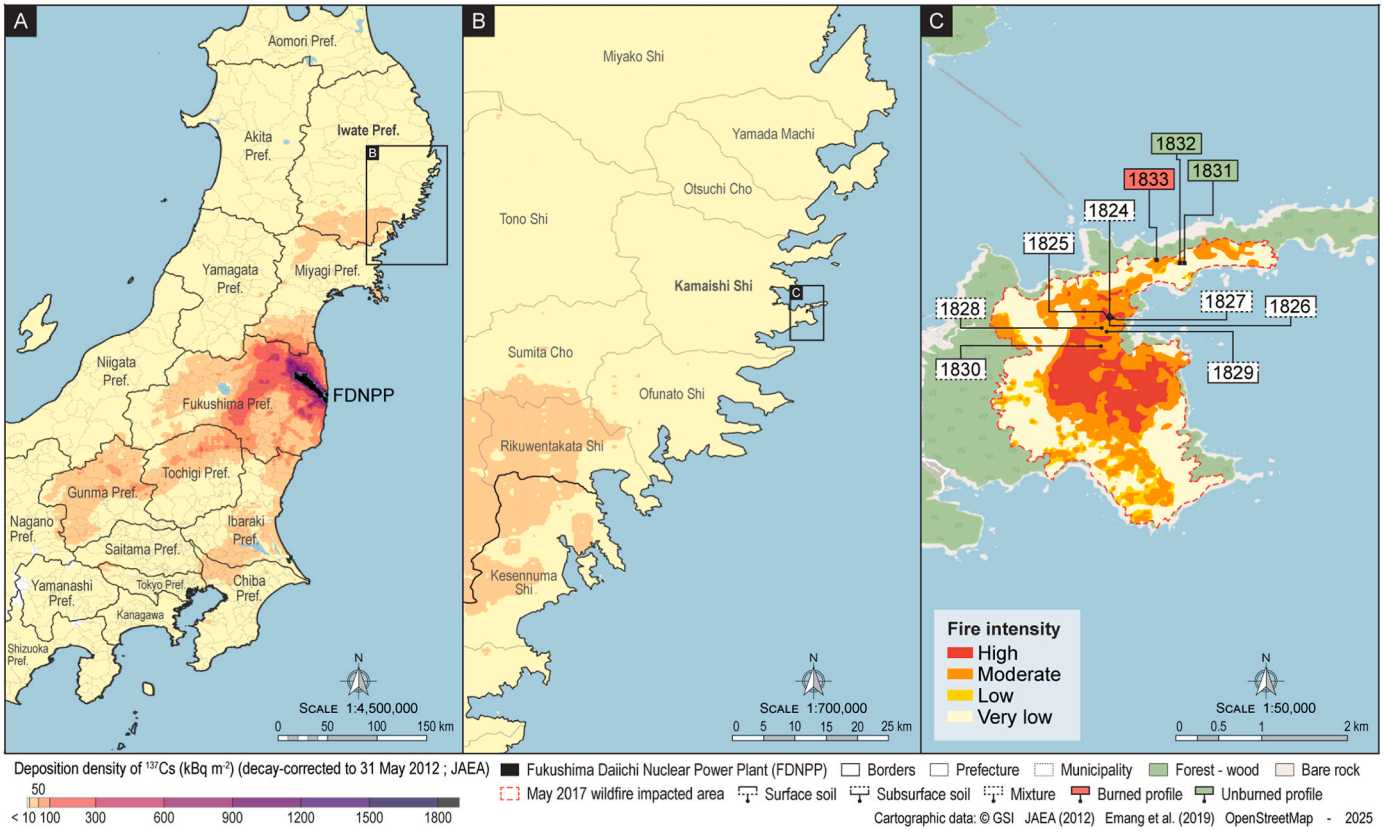

Fig. 1. Deposition density of ^{137}Cs across (**a**) Northeastern Japan and (**b**) southeastern Iwate Prefecture following FDNPP accident according to the airborne monitoring survey conducted by the prefecture and decay-corrected to May 31, 2012 (JAEA, 2012), and the (**c**) fire intensity and impacted area by the wildfire of May 2017 (Emang et al., 2019), with the location of soil and sediment samples and soil profiles analysed in the current research.

2. Materials and methods

2.1. Study area

Burned areas in Kamaishi were covered with both planted and natural trees. Planted forests mainly consisted of conifers, such as *Pinus densiflora* and *Cryptomeria japonica*, and natural forests typically included broadleaf trees such as *Castanea* and *Quercus serrata* (Touge et al., 2018). The burned area is dominated by Brown Forest soils (Obara et al., 2011, 2015), equivalent to Haplic Cambisols in the World Reference Base, and is mainly underlied by hard chert and slate (Irasawa M. et al., 2020). Annual average precipitation and temperature in Kamaishi during the 1991–2020 period amounted to 1693 mm and 11.7 °C, respectively (JMA, 2025). This region is prone to wildfires during dry spring, and several large wildfires have occurred previously in the area (e.g., April 1987 and April 2008) (Touge et al., 2018).

According to the airborne monitoring survey conducted in the Iwate Prefecture late in 2012, the deposition density of ^{137}Cs in the burned area was below 10 kBq m^2 (measurement limit; Fig. 1b). Nonetheless, a higher deposition density of ^{137}Cs (10–50 kBq m^2) was found close to the investigated area, about 40 km to the southwest.

Two types of soil samples were collected in autumn in 2023 in the zone located nearby Kamaishi City and affected by the wildfire of May 2017 (Fig. 1b–c).

2.2. Grab soil surface samples

Seven grab soil surface samples were collected on October 31, 2023 (Fig. 1c). Care was taken to collect the 0–2 cm uppermost soil material in areas connected to the drainage network using a plastic trowel. To this end, the surface scarce vegetation cover was carefully removed with a scraping plate to define the '0-cm' level, and the uppermost 2-cm layer of the soil was collected after marking out the exact area and depth to be collected with the plate and a measuring tape. In total, 5 to 10 subsamples of ca. 10 g were collected within a radius of 5 m and well-mixed in a plastic bag. Samples were collected to characterize both surface material (i.e., soil in forested areas before the fire; n = 3) vs. subsurface material (i.e., soil from rills and gullies incising the hillslope down to more than 5 cm depth; n = 2) that may supply sediment transiting flow concentration pathways across the hillslopes. Such sediment was collected (n = 2) in a flow concentration pathway draining the potential sources.

2.3. Depth-incremented soil profiles

The fire severity map produced by Emang et al. (2019) and relying on a field survey and the detection of changes in Normalized Difference Vegetation Index (NDVI) due to the 2017 wildfire was used to select the sampling locations of the current research. Three pits were dug with a shovel on November 1, 2023 to collect depth-incremented soil profiles in an area affected by the 2017 wildfire (n = 1) and in an unaffected zone (n = 2) (Fig. 1c). Then, 5 cm-increment samples were taken down to a depth of 15–20 cm. Such 5-cm depth increments were also collected in the soil pits investigated under forests all across Japan in the framework of the National Forest Soil Carbon Inventory (NFSCI) project (Ito et al., 2020). Along each profile, soil bulk density was determined with the entire oven-dry mass of successive soil core samples collected every 5-cm increments divided by the volume of the coring device.

2.4. Gamma spectrometry analyses

Samples were oven-dried for 48 h at 50 °C and sieved to 2 mm. They were then prepared in 60 mL polyethylene containers and analysed for 24–48 h using low-background planar-type hyperpure Germanium gamma spectrometry detectors to allow the detection of traces of ^{134}Cs along with that of the more abundant ^{137}Cs. Activities in ^{137}Cs were determined using the characteristic emission peak at 662 keV, while for ^{134}Cs they were calculated as the mean of activities measured at both 604 and 795 keV. For $^{210}Pb_{xs}$ activities, they were calculated by subtracting the supported activity (determined by using two ^{226}Ra daughters including ^{214}Pb activities [through the average count number at 295.2 and 351.9 keV] and ^{214}Bi activity [609.3 keV]) from the total ^{210}Pb activity measured at 46.5 keV. All activities were decay-corrected to the sampling date (i.e., October 31, 2023 or November 1, 2023). Quality assurance was carried out through the analysis of certified International Atomic Energy Agency (IAEA) reference materials (e.g., IAEA-444, IAEA-375) analysed in the same conditions as the samples investigated in the current research.

2.5. Estimation of post-accidental radiocesium deposition

To estimate the initial fallout at the time of FDNPP accident, radiocesium activities in samples were also decay-corrected to March 15, 2011 (i.e. period of estimated maximum radioactive fallout on land in Northeastern Japan).

Radionuclide inventories (I; Bq m^{-2}) were then calculated for each profile following Eq. (1).

$$I = \sum_{k=0}^{n} A*BD*1000*0.05 \quad (1)$$

Where n is the number of successive 0.05 m depth increments of the profile; A is the fallout radionuclide activity in Bq kg^{-1} and BD is the bulk density in g cm^{-3}.

These inventory values were compared to the maps available from airborne surveys and the literature (Ito et al., 2020; Kato et al., 2019).

3. Results and discussion

3.1. Fallout radionuclide activities in grab soil samples

At the time of sampling, all the samples collected showed significant activities in $^{210}Pb_{xs}$ and ^{137}Cs (Fig. 2), although ^{134}Cs activities remained below the detection limits (<0.5 Bq kg^{-1}) in all samples except in one sediment sample collected in the flow concentration pathway (0.6 Bq kg^{-1}). Furthermore, ^{137}Cs activities appeared to be much higher in surface material (range: 1.7 ± 0.3–29.6 ± 1.0 Bq kg^{-1}) compared to subsurface material (range: below detection limit – 1.6 ± 0.4 Bq kg^{-1}), the activities found in sediment lying between those found in both potential source types (range: 3.2 ± 0.2–10.3 ± 0.7 Bq kg^{-1}). Accordingly, ^{137}Cs activities may potentially be used as a tracer to quantify surface vs. subsurface source contributions to sediment, even in such a disturbed environment after a wildfire. The virtual absence of ^{134}Cs in the samples may be due to the low quantities of this radioisotope deposited in the region after Fukushima accident, or to its rapid erosion and transfer to lower locations since the deposition period, as erosion is known to be accelerated in burned areas following wildfires (Wilkinson et al., 2009). It is also known that most (>86 %) of ^{134}Cs was concentrated in the uppermost 2 cm of the soil following the accident (Kato et al., 2012; Lepage et al., 2014), which made it particularly exposed to potential erosion.

In contrast, $^{210}Pb_{xs}$ activities were found in all samples (range: 10 ± 3.9–72 ± 5.5 Bq kg^{-1}), without clear differences related to the sample type. This result is likely due to continuous supply of this radionuclide through rainfall, as ^{210}Pb is a natural radionuclide, which contrasts from the situation observed for ^{137}Cs in Japan, which was only supplied following atmospheric nuclear bomb testing in the 1960s and FDNPP accident in 2011 (Ito et al., 2020).

3.2. Fallout radionuclide activities in soil depth profiles

The three fallout radionuclides of interest (^{134}Cs, ^{137}Cs, $^{210}Pb_{xs}$) were

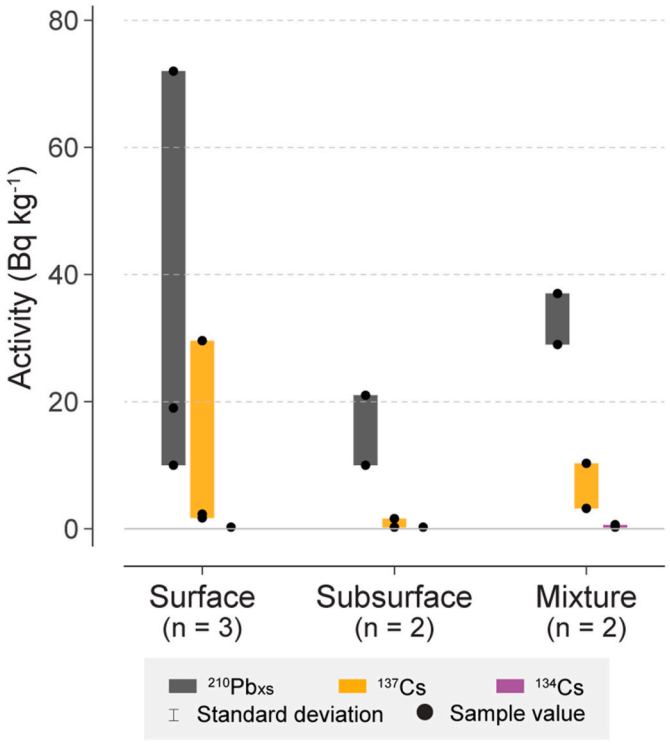

Fig. 2. Fallout radionuclide activities and range decay-corrected to the sampling date of grab soil samples and sediment collected across a burned hillslope of Kamaishi, Japan.

all detected in the three collected profiles. Among them, ^{134}Cs was only detected in the uppermost depth increment (0–5 cm), with activities ranging from 2.0 ± 0.4 Bq kg^{-1} to 3.2 ± 0.6 Bq kg^{-1}. A clear decrease in activities with depth was observed for the other radionuclides. First, ^{137}Cs showed the highest activities in the uppermost depth increment (range: 126 ± 2.2174 ± 2.2 Bq kg^{-1}) compared to those observed at higher depths. Of note, ^{137}Cs was detected between 10 and 15 cm depths, although in much lower activities (range: 7 ± 0.6–28 ± 0.9 Bq kg^{-1}). Similar findings were obtained for ^{210}Pb$_{xs}$, with the highest activities measured between 0 and 5 cm depth (range: 134 ± 7.2 – 257 ± 9.9 Bq kg^{-1}) and much lower values were found between 10 and 15 cm depth (range: <9.0–47 ± 5.0 Bq kg^{-1}). This type of profile showing a continuous decrease of ^{137}Cs concentrations with depth is widely observed in the literature (Jagercikova et al., 2014).

The higher variability observed for ^{210}Pb$_{xs}$ compared to ^{137}Cs may reflect higher concentration of ^{210}Pb$_{xs}$ in surface vegetation and litter as well as the variability of fallout due to heterogeneities in rainfall and vegetation cover (Smith et al., 2012). Interestingly and for all radionuclides investigated, higher values were measured in the profile collected in the burned area compared to those sampled in unaffected areas. This was also observed in studies investigating fallout radionuclides in burned areas of Australia and Spain, given all the radionuclides intercepted by the vegetation are concentrated and incorporated in the ash produced by the wildfire (García-Comendador et al., 2017; Smith et al., 2012). The variability of fallout radionuclide inventories in soils under forests was also documented in Japan although not in post-wildfire conditions, with coefficients of variability of 5–48 % for ^{137}Cs and 14–51 % for ^{210}Pb$_{xs}$ observed for a site of Shikoku Island (Wakiyama et al., 2010). Such a high variability of ^{210}Pb$_{xs}$ activities that are continuously supplied to the soils was also found in a study comparing radionuclides along contrasted soil profiles collected in long term experiments around the world, and it demonstrated the occurrence of higher activities in the litter layer than in the organo-mineral horizons (de Tombeur et al., 2020). Furthermore, as the occurrence of a linear relationship has been found between ^{210}Pb$_{xs}$ annual deposits and the annual amount of rainfall (Baskaran, 2011) and as rainfall is known to show strong spatial heterogeneities in mountainous environments (Laceby et al., 2016) as in the study area, this factor can also explain the higher variability observed for ^{210}Pb$_{xs}$.

As the analyses conducted in the framework of the current research were conducted 6 years after the event, it is also possible that some post-fire disturbances associated with rainfall, overland flow or wind took place before sampling was achieved, which may have increased the variability of radionuclide activities along the profile. For instance, García-Comendador et al. (2017) demonstrated the dominant impact of the first rainfall events that occur after the wildfire on soil erosion and associated radionuclide transfers.

3.3. Estimation of post-accidental radiocesium deposition

When they are decay-corrected to the main fallout period estimated to have taken place after FDNPP accident (i.e., March 15, 2011), ^{134}Cs activities detected in the uppermost layers of the soil profiles range between 150 and 226 Bq kg^{-1}, which corresponds to 64–98 % of the ^{137}Cs activities detected in the same layers. It can therefore be inferred that most of the radiocesium detected in soils of the region was supplied by FDNPP accident rather than by the atmospheric nuclear bomb testing in the 1960s. This is consistent with the analysis of samples collected in agricultural land between 2007 and 2010 in Fukushima Prefecture located in the Tohoku Region of Japan, which showed that only 3.1–5.0 Bq kg^{-1} of ^{137}Cs was found in these soils before the additional inputs related to the accident (Jaegler et al., 2019).

In terms of radionuclide inventories (Fig. 3), at the time of sampling, ^{137}Cs inventories in both unburned profiles amounted to 6.0–6.5 kBq m^{-2}, while the corresponding inventory was higher in the burned profile (7.5 kBq m^{-2}), which was expected as it includes the fallout incorporated in above-ground vegetation and reduced into ash due to the wildfire. A similar finding is made for ^{210}Pb$_{xs}$ inventories (as it was similar in both unburned profiles – 6.2 to 6.8 kBq m^{-2} – while higher in the burned profile with 10.7 kBq m^{-2}) (Smith et al., 2012). When decay-correcting ^{134}Cs inventories to the initial FDNPP fallout period (i.e., March 15, 2011), values comprised between 3.1 and 5.6 kBq m^{-2} are found for the three profiles, representing 37–64 % of the total radiocesium profile inventories, which remains consistent with the interpretation made based on radionuclide activities. The values found in the current research are also close to those reported by Tagami et al. (2019) who found 3.6 kBq m^{-2} of ^{137}Cs by 2019 at Akita City located at a similar latitude as Kamaishi, in Japan.

Although the ^{137}Cs initial fallout map reconstruction made by Kato et al. (2019) does not cover Iwate Prefecture, it does include the nearby Miyagi Prefecture. In the part of Miyagi Prefecture located the closest to the current study site, a fallout 'hotspot' with values comprised between 5 and 10 kBq m^{-2} is predicted, which is consistent with the values found in the current research (~8 kBq m^{-2} of ^{137}Cs by March 2011). These values > 5 kBq m^{-2} exceed significantly those predicted for global fallout in this region by Ito et al. (2020). Accordingly, the occurrence of significant Fukushima-related fallout in 2011, roughly of the same order of magnitude as the global fallout associated with the nuclear atmospheric tests that took mainly place in the 1960s, therefore requires to be considered when interpreting radionuclide data in environmental samples collected during the last 15 years in Northeastern Japan.

4. Conclusions

To the best of our knowledge, the current research showed for the first time the occurrence of FDNPP accident-related radiocesium deposition in soils of Iwate Prefecture (Tohoku Region, Northeastern Japan). Furthermore, it demonstrated through the detection of traces of ^{134}Cs that may only have been supplied to the environment in Japan by FDNPP accident during the 21st century that this event supplied at least

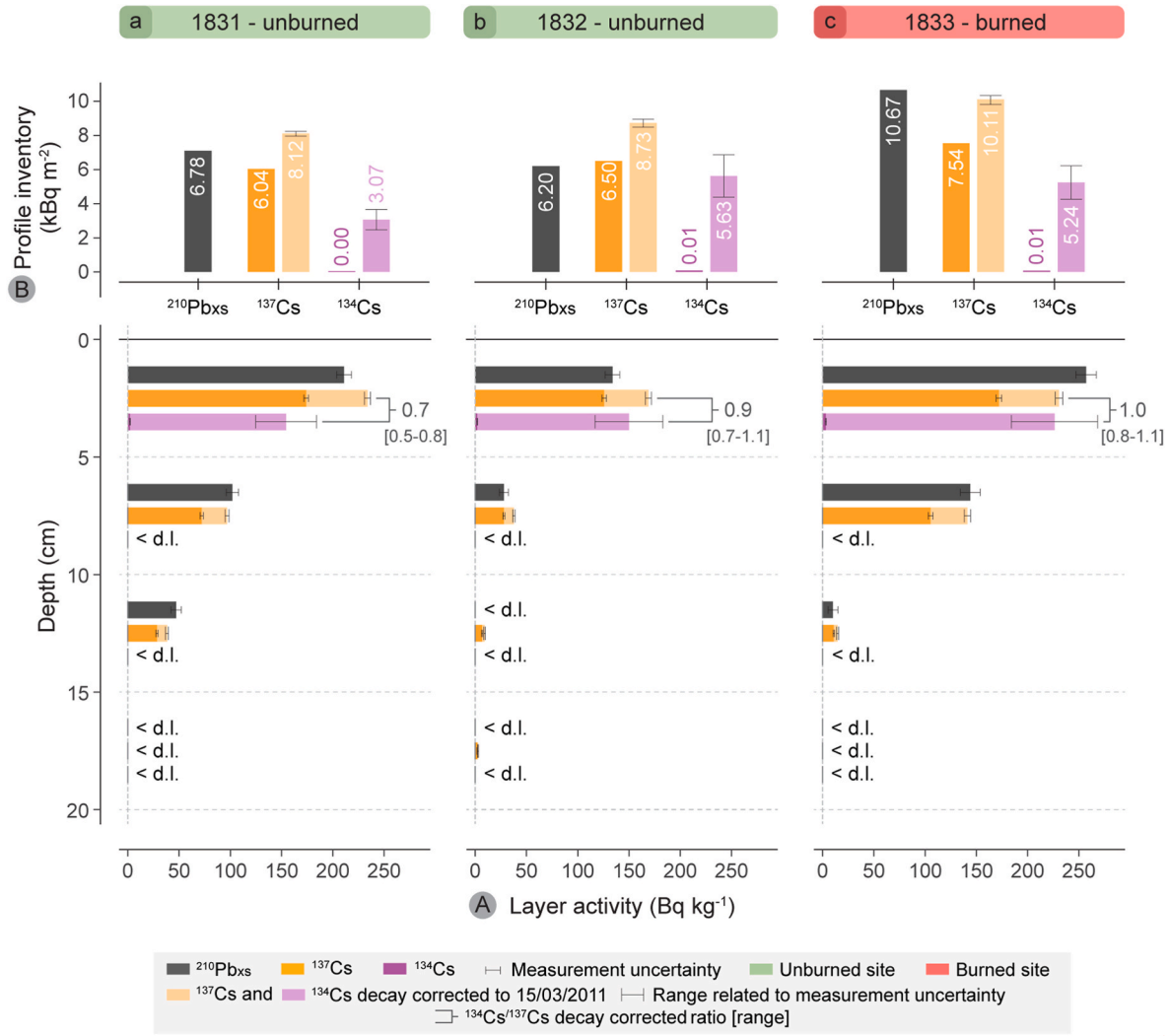

Fig. 3. Fallout radionuclide inventories and activities (decay-corrected to the sampling date and to the FDNPP fallout date) measured with depth in soil profiles collected in Kamaishi in unaffected areas by the 2017 wildfire [profiles (a) and (b)] and in a burned area [profile (c)]. "< d.l." refers to measurements below the detection limit of about 0.5 Bq kg^{-1}.

as much radiocesium as global fallout associated with the nuclear atmospheric tests to the soils of the region. Although the sample number does not capture the full spatial heterogeneity of fallout across the region, it is sufficient to demonstrate the presence, magnitude and vertical distribution of Fukushima-derived radiocesium. This finding is important for future research relying on artificial fallout radionuclides as chronological markers in the region such as those establishing age models of sediment archives based on radionuclide depth profiles. As for the use of radionuclides as tracers of sediment source contributions across landscapes in this part of Northeastern Japan, our results confirming the enrichment of surface sources in ^{137}Cs vs. the depletion of subsoil sources in ^{137}Cs show that this radionuclide may provide a useful marker to distinguish these sediment source contributions, even in post-wildfire conditions. Nevertheless, the fact that a significant proportion of the radiocesium detected nowadays in soils of this region was supplied by FDNPP accident should be considered when interpreting the results in terms of process dynamics with time. In the near future, soil samples that may be useful for environmental research conducted in the region could be analysed for ^{134}Cs as long as it remains detectable (i.e. by 2031) to facilitate future interpretations that will be more complex when ^{137}Cs alone will be measurable.

CRediT authorship contribution statement

Olivier Evrard: Writing – original draft, Resources, Formal analysis, Conceptualization. **Naoya Takahashi:** Writing – review & editing, Resources, Formal analysis. **Hotaka Sato:** Writing – review & editing, Resources, Formal analysis. **Ryoga Ohta:** Writing – review & editing, Resources, Formal analysis. **Anthony Foucher:** Writing – review & editing, Resources, Formal analysis. **Thomas Chalaux-Clergue:** Writing – review & editing, Visualization, Resources, Formal analysis. **Pierre-Alexis Chaboche:** Writing – review & editing, Resources, Formal analysis.

Declaration of competing interest

The authors declare that they have no known competing financial interests or personal relationships that could have appeared to influence the work reported in this paper.

Acknowledgements

This work has been supported by the *French National Centre of Scientific Research* (CNRS) and the *French Atomic Energy Commission* (CEA) in the framework of MITATE Lab. Thomas Chalaux-Clergue (PE22708)

and Pierre-Alexis Chaboche also received support from the *Japanese Society for the Promotion of Science* (JSPS).

Data availability

All metadata and data are available (https://doi.org/10.5281/zenodo.17607454) on Zenodo (Evrard et al., 2025).

References

Baskaran, M., 2011. Po-210 and Pb-210 as atmospheric tracers and global atmospheric Pb-210 fallout: a review. J. Environ. Radioact. 102, 500–513.

Bruel, R., Sabatier, P., 2020. Serac: a R package for ShortlivEd RAdionuclide chronology of recent sediment cores. J. Environ. Radioact. 225.

de Tombeur, F., Cornu, S., Bourlès, D., Duvivier, A., Pupier, J., Aster, T., Brossard, M., Evrard, O., 2020. Retention of ^{10}Be, ^{137}Cs and ^{210}Pb$_{xs}$ in soils: Impact of physico-chemical characteristiis. Geoderma 367.

Emang, G.P., Touge, Y., Kazama, S., 2019. Assessing NDVI based phenology in different fire severity in the Kamaishi 2017 Forest fire. Journal of Japan Society of Civil Engineers, Ser. G (Environmental Research) 75–5, I_135–I_140.

Estrany, J., López-Tarazón, J.A., Smith, H.G., 2016. Wildfire effects on suspended sediment delivery quantified using fallout radionuclide tracers in a mediterranean catchment. Land Degrad. Dev. 27, 1501–1512.

Evrard, O., Chaboche, P.-A., Ramon, R., Foucher, A., Laceby, J.P., 2020. A global review of sediment source fingerprinting research incorporating fallout radiocesium (^{137}Cs). Geomorphology 362, 107103.

Evrard, O., Chalaux-Clergue, T., Takahashi, N., Chaboche, P.-A., Sato, H., Ohta, R., Foucher, A., 2025. Fallout radionuclide activities and inventories in the area affected by the 2017 wildfire in Kamaishi (Iwate Prefecture, Tohoku Region, Japan). Zenodo. https://doi.org/10.5281/zenodo.17607454 [Data set].

Evrard, O., Laceby, J.P., Lepage, H., Onda, Y., Cerdan, O., Ayrault, S., 2015. Radiocesium transfer from hillslopes to the Pacific Ocean after the Fukushima Nuclear Power Plant accident: a review. J. Environ. Radioact. 148, 92–110.

Foucher, A., Chaboche, P.-A., Sabatier, P., Evrard, O., 2021. A worldwide meta-analysis (1977–2020) of sediment core dating using fallout radionuclides including ^{137}Cs and ^{210}Pb$_{xs}$. Earth Syst. Sci. Data 13, 4951–4966.

García-Comendador, J., Fortesa, J., Calsamiglia, A., Garcias, F., Estrany, J., 2017. Source ascription in bed sediments of a Mediterranean temporary stream after the first post-fire flush. J. Soils Sediments 17, 2582–2595.

Hori, M., Saito, T., Shozugawa, K., 2018. Source evaluation of ^{137}Cs in foodstuffs based on trace ^{134}Cs radioactivity measurements following the Fukushima nuclear accident. Sci. Rep. 8, 16806.

Irasawa, M., Matsuo, S., Arai, M., Kainori, M., Tsou, C.-Y., Yamada, T., Kasai, M., Koi, T., Kato, N., Wakahara, T., Higaki, D., Ikeda, H., Ishikawa, Y., Arai, K., Hirose, S., Sato, T., Kawatabata, H., Koubu, M., Niwa, S., et al., 2020. Sediment disasters caused by Typhoon Hagibis on October, 2019 in Tohoku region (No. 6). J. Japan Soc. Erosion Control Eng. 13 (2), 48–55.

Ito, E., Miura, S., Aoyama, M., Shichi, K., 2020. Global ^{137}Cs fallout inventories of forest soil across Japan and their consequences half a century later. J. Environ. Radioact. 225, 106421.

JAEA, 2012. Results of Deposition of Radioactive Cesium of the Airborne Monitoring Survey by Prefecture (Decay correction: may 31, 2012). https://emdb.jaea.go.jp/emdb_old/en/portals/b1020201/.

Jaegler, H., Pointurier, F., Diez-Fernandez, S., Gourgiotis, A., Isnard, H., Hayashi, S., Tsuji, H., Onda, Y., Hubert, A., Laceby, J.P., Evrard, O., 2019. Reconstruction of uranium and plutonium isotopic signatures in sediment accumulated in the Mano Dam reservoir, Japan, before and after the Fukushima nuclear accident. Chemosphere 225, 849–858.

Jaegler, H., Pointurier, F., Onda, Y., Hubert, A., Laceby, J.P., Cirella, M., Evrard, O., 2018. Plutonium isotopic signatures in soils and their variation (2011-2014) in sediment transiting a coastal river in the Fukushima Prefecture, Japan. Environ. Pollut. 240, 167–176.

Jagercikova, M., Cornu, S., Le Bas, C., Evrard, O., 2014. Vertical distributions of ^{137}Cs in soils: a meta-analysis. J. Soils Sediments 15, 81–95.

JMA, 2025. https://www.data.jma.go.jp/stats/etrn/index.php?prec_no=33&block_no=0233&year=&month=&day=&view=.

Kato, H., Onda, Y., Gao, X., Sanada, Y., Saito, K., 2019. Reconstruction of a Fukushima accident-derived radiocesium fallout map for environmental transfer studies. J. Environ. Radioact. 210, 105996.

Kato, H., Onda, Y., Teramage, M., 2012. Depth distribution of ^{137}Cs, ^{134}Cs, and ^{131}I in soil profile after Fukushima Dai-ichi Nuclear Power Plant Accident. J. Environ. Radioact. 111, 59–64.

Kobayashi, S., Shinomiya, T., Kitamura, H., Ishikawa, T., Imaseki, H., Oikawa, M., Kodaira, S., Miyaushiro, N., Takashima, Y., Uchihori, Y., 2015. Radioactive contamination mapping of northeastern and eastern Japan by a car-borne survey system, Radi-Probe. J. Environ. Radioact. 139, 281–293.

Laceby, J.P., Chartin, C., Evrard, O., Onda, Y., Garcia-Sanchez, L., Cerdan, O., 2016. Rainfall erosivity in catchments contaminated with fallout from the Fukushima Daiichi nuclear power plant accident. Hydrol. Earth Syst. Sci. 20, 2467–2482.

Lepage, H., Evrard, O., Onda, Y., Lefèvre, I., Laceby, J.P., Ayrault, S., 2014. Depth distribution of radiocesium in Fukushima paddy fields and implications for ongoing decontamination works. SOIL Discussions 1, 401–428.

Mabit, L., Benmansour, M., Walling, D.E., 2008. Comparative advantages and limitations of the fallout radionuclides ^{137}Cs, ^{210}Pb$_{ex}$ and ^{7}Be for assessing soil erosion and sbdimentation. J. Environ. Radioact. 99, 1799–1807.

Magre, A., Boulet, B., Pourcelot, L., Roy-Barman, M., de Vismes Ott, A., Ardois, C., 2022. Improved radiocesium purification in low-level radioactive soil and sediment samples prior to ^{135}Cs/^{137}Cs ratio measurement by ICP-MS/MS. J. Radioanal. Nucl. Chem. 331, 4067–4076.

Masson, O., Baeza, A., Bieringer, J., Brudecki, K., Bucci, S., Cappai, M., Carvalho, F.P., Connan, O., Cosma, C., Dalheimer, A., Didier, D., Depuydt, G., De Geer, L.E., De Vismes, A., Gini, L., Groppi, F., Gudnason, K., Gurriaran, R., Hainz, D., Halldorsson, O., Hammond, D., Hanley, O., Holey, K., Homoki, Z., Ioannidou, A., Isajenko, K., Jankovic, M., Katzlberger, C., Kettunen, M., Kierepko, R., Kontro, R., Kwakman, P.J., Lecomte, M., Leon Vintro, L., Leppanen, A.P., Lind, B., Lujaniene, G., Mc Ginnity, P., Mc Mahon, C., Mala, H., Manenti, S., Manolopoulou, M., Mattila, A., Mauring, A., Mietelski, J.W., Moller, B., Nielsen, S.P., Nikolic, J., Overwater, R.M., Palsson, S.E., Papastefanou, C., Penev, I., Pham, M.K., Povinec, P.P., Rameback, H., Reis, M.C., Ringer, W., Rodriguez, A., Rulik, P., Saey, P.R., Samsonov, V., Schlosser, C., Sgorbati, G., Silobritiene, B.V., Soderstrom, C., Sogni, R., Solier, L., Sonck, M., Steinhauser, G., Steinkopff, T., Steinmann, P., Stoulos, S., Sykora, I., Todorovic, D., Tooloutalaie, N., Tositti, L., Tschiersch, J., Ugron, A., Vagena, E., Vargas, A., Wershofen, H., Zhukova, O., 2011. Tracking of airborne radionuclides from the damaged Fukushima Dai-ichi nuclear reactors by European networks. Environ. Sci. Technol. 45, 7670–7677.

Meusburger, K., Evrard, O., Alewell, C., Borrelli, P., Cinelli, G., Ketterer, M., Mabit, L., Panagos, P., van Oost, K., Ballabio, C., 2020. Plutonium aided reconstruction of caesium atmospheric fallout in European topsoils. Sci. Rep. 10, 11858.

Obara, H., Maejima, Y., Kohyama, K., Ohkura, T., Takata, Y., 2015. Outline of the comprehensive soil classification System of Japan – first approximation. Jpn. Agric. Res. Q. 49, 217–226.

Obara, H., Ohkura, T., Takata, Y., Kohyama, K., Maejima, Y., Hamazaki, T., 2011. Comprehensive Soil Classification System of Japan First Approximation. Nogyo Kankyo Gijutsu Kenkyusho Hokoku = Bulletin of National Institute for Agro-Environmental Sciences, pp. 1–37.

Onda, Y., Taniguchi, K., Yoshimura, K., Kato, H., Takahashi, J., Wakiyama, Y., Coppin, F., Smith, H., 2020. Radionuclides from the Fukushima Daiichi Nuclear Power Plant in terrestrial systems. Nat. Rev. Earth Environ. 1, 644–660.

Owens, P.N., 2020. Soil erosion and sediment dynamics in the Anthropocene: a review of human impacts during a period of rapid global environmental change. J. Soils Sediments 20, 4115–4143.

Shozugawa, K., Nogawa, N., Matsuo, M., 2012. Deposition of fission and activation products after the Fukushima Dai-ichi nuclear power plant accident. Environ. Pollut. 163, 243–247.

Smith, H.G., Sheridan, G.J., Lane, P.N.J., Noske, P.J., Heijnis, H., 2011. Changes to sediment sources following wildfire in a forested upland catchment, southeastern Australia. Hydrol. Process. 25, 2878–2889.

Smith, H.G., Sheridan, G.J., Nyman, P., Child, D.P., Lane, P.N.J., Hotchkis, M.A.C., Jacobsen, G.E., 2012. Quantifying sources of fine sediment supplied to post-fire debris flows using fallout radionuclide tracers. Geomorphology 139–140, 403–415.

Steinhauser, G., 2014. Fukushima's forgotten radionuclides: a review of the understudied radioactive emissions. Environ. Sci. Technol. 48, 4649–4663.

Steinhauser, G., Brandl, A., Johnson, T.E., 2014. Comparison of the Chernobyl and Fukushima nuclear accidents: a review of the environmental impacts. Sci. Total Environ. 470–471, 800–817.

Tagami, K., Tsukada, H., Uchida, S., 2019. Quantifying spatial distribution of ^{137}Cs in reference site soil in Asia. Catena 180, 341–345.

Touge, Y., Emang, G.P., Kazama, S., Takahashi, Y., Sasaki, K., 2018. Introduction of the tohoku Forest fires on May 2017; case in Kamaishi city of Iwate prefecture and Kurihara city of Miyagi prefecture. Japan soc. Nat. Disaster Sci. 36, 361–370.

Touge, Y., Hasegawa, M., Minegishi, M., Kawagoe, S., Kazama, S., 2023. Multitemporal UAV surveys of geomorphological changes caused by postfire heavy rain in Kamaishi city, northeast Japan. Catena 220.

Wakiyama, Y., Onda, Y., Mizugaki, S., Asai, H., Hiramatsu, S., 2010. Soil erosion rates on forested mountain hillslopes estimated using ^{137}Cs and ^{210}Pb$_{ex}$. Geoderma 159, 39–52.

Wilkinson, S.N., Wallbrink, P.J., Hancock, G.J., Blake, W.H., Shakesby, R.A., Doerr, S.H., 2009. Fallout radionuclide tracers identify a switch in sediment sources and transport-limited sediment yield following wildfire in a eucalypt forest. Geomorphology 110, 140–151.